

see commentary on page 269

# Hypoxia-inducible factor-2 $\alpha$ -expressing interstitial fibroblasts are the only renal cells that express erythropoietin under hypoxia-inducible factor stabilization

Alexander Paliege<sup>1</sup>, Christian Rosenberger<sup>2</sup>, Anja Bondke<sup>3</sup>, Lina Sciesielski<sup>3</sup>, Ahuva Shina<sup>4</sup>, Samuel N. Heyman<sup>4</sup>, Lee A. Flippin<sup>5</sup>, Michael Arend<sup>5</sup>, Stephen J. Klaus<sup>5</sup> and Sebastian Bachmann<sup>1</sup>

<sup>1</sup>Department of Anatomy, Charité, Berlin, Germany; <sup>2</sup>Department of Nephrology and Medical Intensive Care, Charité, Berlin, Germany; <sup>3</sup>Department of Physiology, Charité, Berlin, Germany; <sup>4</sup>Department of Medicine, Hadassah Hospital, Mt Scopus and the Hebrew University Medical School, Jerusalem, Israel and <sup>5</sup>FibroGen Inc., Southern San Francisco, San Francisco, California, USA

The adaptation of erythropoietin production to oxygen supply is determined by the abundance of hypoxia-inducible factor (HIF), a regulation that is induced by a prolyl hydroxylase. To identify cells that express HIF subunits (HIF-1 $\alpha$  and HIF-2 $\alpha$ ) and erythropoietin, we treated Sprague–Dawley rats with the prolyl hydroxylase inhibitor FG-4497 for 6 h to induce HIF-dependent erythropoietin transcription. The kidneys were analyzed for colocalization of erythropoietin mRNA with HIF-1 $\alpha$  and/or HIF-2 $\alpha$  protein along with cell-specific identification markers. FG-4497 treatment strongly induced erythropoietin mRNA exclusively in cortical interstitial fibroblasts. Accumulation of HIF-2 $\alpha$  was observed in these fibroblasts and in endothelial and glomerular cells, whereas HIF-1 $\alpha$  was induced only in tubular epithelia. A large proportion (over 90% in the juxtamedullary cortex) of erythropoietin-expressing cells coexpressed HIF-2 $\alpha$ . No colocalization of erythropoietin and HIF-1 $\alpha$  was found. Hence, we conclude that in the adult kidney, HIF-2 $\alpha$  and erythropoietin mRNA colocalize only in cortical interstitial fibroblasts, which makes them the key cell type for renal erythropoietin synthesis as regulated by HIF-2 $\alpha$ .

*Kidney International* (2010) **77**, 312–318; doi:10.1038/ki.2009.460; published online 16 December 2009

KEYWORDS: erythropoietin; hypoxia; intracellular signal; intrinsic renal cell; renal physiology

Erythropoietin (EPO) is the principal regulator of red blood cell production, linking decreased tissue oxygenation to an adequate erythropoietic response. The adult kidney accounts for ~90% of the total EPO response, indicating that its expression is under tight, tissue-specific regulation.<sup>1</sup> In this study, the critical importance of hypoxia-inducible transcription factors (HIFs) has been well established. HIFs are heterodimeric transcriptional regulators consisting of distinct oxygen-sensitive  $\alpha$ -subunits (such as HIF-1 $\alpha$ , HIF-2 $\alpha$ , or HIF-3 $\alpha$ ) and a common, stable  $\beta$ -subunit.<sup>2</sup> The oxygen sensitivity of HIFs depends on the action of HIF prolyl hydroxylases (HIF-PHD), which catalyze hydroxylation of proline residues of HIF- $\alpha$  when molecular oxygen is available as a substrate.<sup>3</sup> Hydroxylated HIF- $\alpha$  is recognized by the von Hippel Lindau protein to induce proteasomal degradation.<sup>4</sup> Under hypoxia, degradation is inhibited and HIF- $\alpha$  can be transferred to the nucleus where it recruits HIF- $\beta$  and the transcriptional coactivator p300 for its activation.<sup>2</sup> In addition to molecular oxygen, HIF-PHD activity depends on the availability of 2-oxoglutarate, ferrous iron, and ascorbate as cofactors. Pharmacological interference with any of these cofactors has been shown to impair oxygen-dependent HIF degradation.<sup>5–7</sup> In this study, we used the 2-oxoglutarate analog, FG-4497, to inhibit HIF-PHDs. This compound has been shown by us and others to enhance the nuclear abundance of HIF isoforms, to induce the expression of HIF target genes such as EPO, and to increase its plasma levels without apparent toxicity.<sup>8–11</sup>

Available data obtained from cell models and transgenic mice have provided evidence for HIF-1 $\alpha$  and HIF-2 $\alpha$  to contribute to the stimulation of EPO-mRNA expression at least under certain conditions.<sup>12–17</sup> In the adult organism, renal EPO expression seems to be preferentially regulated by HIF-2 $\alpha$  and not by HIF-1 $\alpha$ .<sup>14,17–19</sup> Previous work has defined the localization of EPO synthesis in a subset of cortical interstitial fibroblasts, which are characterized by their

**Correspondence:** Sebastian Bachmann, Charité - Universitätsmedizin Berlin, Institut für Vegetative Anatomie, Philippstr. 12, Berlin 10115, Germany.  
E-mail: sbachm@charite.de

Received 8 January 2009; revised 12 August 2009; accepted 30 September 2009; published online 16 December 2009

expression of ecto-5'-nucleotidase (5'NU).<sup>20–25</sup> In agreement with the proposed role of HIF-2 $\alpha$  in EPO activation, we have shown earlier that only HIF-2 $\alpha$  was expressed in cells of the renal cortical interstitium.<sup>8,26–28</sup> In contrast, HIF-1 $\alpha$  was distributed in tubular epithelia.<sup>8,27,28</sup> This would imply cellular colocalization of HIF-2 $\alpha$  and EPO upon adequate activation; to date, however, this has not been shown. In addition, the identity of HIF-2 $\alpha$ -expressing cortical interstitial cells remains to be defined. Therefore, we applied FG-4497 in rats as a suitable approach to increase HIF- $\alpha$  abundance and resulting EPO mRNA expression to resolve this issue.

## RESULTS

The renal distribution of EPO mRNA signal as well as that of HIF-1 $\alpha$ - and HIF-2 $\alpha$ -immunoreactive signals was determined in rats treated with FG-4497 or vehicle for 6 h (Figure 1a–d). EPO mRNA signal, as shown by *in situ* hybridization, was localized to cortical interstitial cells; positive cells were predominantly found in the cortical labyrinth and to a lesser extent in the medullary rays; epithelial and vascular structures were negative (Figure 1b). Control animals did not show reproducible EPO mRNA staining (Figure 1a). The majority of EPO-expressing cells were located in the juxtamedullary (deep) regions of the renal cortex ( $59 \pm 3$  cells per mm<sup>2</sup>), whereas in the superficial cortex, their distribution was more scarce ( $25 \pm 6$  cells per mm<sup>2</sup>; Table 1). HIF immunoreactivity was principally restricted to the cell nuclei. Staining for HIF-1 $\alpha$  was localized to epithelial cells, whereas nonepithelial cells were negative (Figure 1c); signals were more frequent in the superficial cortex ( $952 \pm 5$  cells per mm<sup>2</sup>) than in the deep cortex ( $642 \pm 7$  cells per mm<sup>2</sup>; Table 1). Cortical HIF-2 $\alpha$  staining in the kidneys of FG-4497-treated rats was localized to interstitial cells and to a number of endothelial and glomerular cells (Figure 1d); interstitial HIF-2 $\alpha$  distribution showed no major difference between deep and superficial cortices ( $123 \pm 21$  vs  $91 \pm 12$  cells per mm<sup>2</sup>; Table 1). Kidney samples obtained from control rats were devoid of HIF- $\alpha$  signals (Table 1). Colocalization of EPO mRNA and HIF- $\alpha$  isoforms was evaluated on mirror sections of the kidney (Figure 2a–h). HIF-1 $\alpha$  immunoreactivity did not show spatial association with EPO mRNA expression (Figure 2a–d). By contrast, HIF-2 $\alpha$  immunoreactivity showed colocalization with EPO mRNA expression in the vast majority of EPO-producing fibroblasts in the superficial and deep regions of the cortex ( $83 \pm 1.4\%$  and  $91 \pm 0.6\%$ , respectively; Figure 2e–h; Table 1).

To identify the nature of labeled interstitial cells in FG-4497-treated rats, we performed double staining for EPO mRNA and the interstitial fibroblast marker, 5'NU. The resulting frequent coexpression of 5'NU immunoreactive signal and EPO mRNA within the same cells confirmed their nature as fibroblasts, corresponding to previous evidence obtained for this cell type under anemic and hypoxic conditions (Figure 3).<sup>20,22,24</sup> In contrast, caveolin-1-immuno-

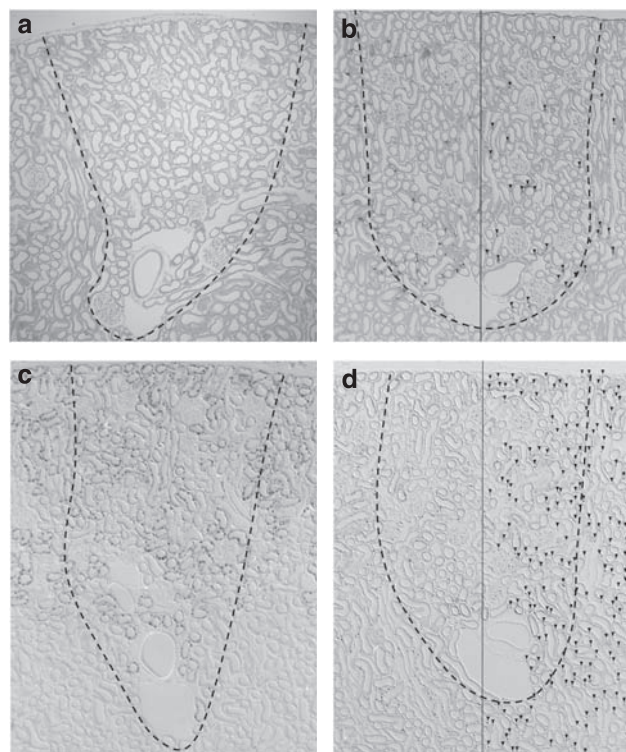


**Figure 1 | Induction of renal EPO, HIF-1 $\alpha$ , and HIF-2 $\alpha$  signals by FG-4497.** (a) Control and (b–d) FG-4497 (FG)-treated tissues are shown. (a) No EPO mRNA signal is detectable in control. (Panel b) EPO mRNA *in situ* hybridization shows intense staining of cortical interstitial cells in FG-treated tissues. Signal density is highest in the juxtamedullary portion (arrowheads on the right side of the vertical bar indicate positive cells). (c) Immunostaining for HIF-1 $\alpha$  shows nuclear staining of cortical tubular cells. The density of HIF-1 $\alpha$ -expressing cells is highest in the superficial half of the renal cortex and decreases toward the cortico-medullary transition. Cortical interstitial cells are negative. (d) Immunostaining for HIF-2 $\alpha$  shows nuclear staining of cortical interstitial cells (arrowheads on the right side indicate positive cells). In addition, staining can be found in the vascular endothelium and glomerular cells. There are no major differences between the juxtamedullary and the subcapsular region of the renal cortex. The cortical labyrinth is marked by dashed lines. Assembled micrographs; original magnification  $\times 100$ . EPO, erythropoietin; HIF, hypoxia-inducible factor.

reactive endothelial cells did not display EPO mRNA signal throughout (Figure 4). To characterize HIF-2 $\alpha$ -expressing interstitial cells, we performed double labeling for HIF-2 $\alpha$  and markers for the cellular constituents of the cortical interstitium. Strong HIF-2 $\alpha$  immunoreactivity was found in the nuclei of cells that also expressed the fibroblast marker 5'NU (Figure 5a–c). We further observed HIF-2 $\alpha$  staining in a subset of nuclei of RECA-1 (rat endothelial cell antigen-1)-positive endothelial cells (Figure 5d–f). Quantitative assessment of interstitial HIF-2 $\alpha$  distribution showed that  $74 \pm 9.7\%$  of the HIF-2 $\alpha$ -immunoreactive nuclei belonged to interstitial fibroblasts and  $25 \pm 5.6\%$  of them to endothelial cells (Table 2). Major histocompatibility complex II-immunoreactive dendritic cells and macrophages did not show HIF-2 $\alpha$  immunostaining (Figure 5g–i; Table 2).

**Table 1 | Quantification of EPO mRNA, HIF-1 $\alpha$ , and HIF-2 $\alpha$  signals**

	VE IC		FG IC		VE tubule		FG tubule	
	Deep	Superficial	Deep	Superficial	Deep	Superficial	Deep	Superficial
EPO (cells per mm <sup>2</sup> $\pm$ s.e.m.)	0	0	59 $\pm$ 2.5	25 $\pm$ 6	0	0	0	0
HIF-1 $\alpha$ (cells per mm <sup>2</sup> $\pm$ s.e.m.)	0	0	0	0	0	0	642 $\pm$ 7.4	952 $\pm$ 5
HIF-2 $\alpha$ (cells per mm <sup>2</sup> $\pm$ s.e.m.)	0	0	123 $\pm$ 21	91 $\pm$ 12	0	0	0	0
EPO+HIF-1 $\alpha$ (% $\pm$ s.e.m.)	0	0	0	0	0	0	0	0
EPO+HIF-2 $\alpha$ (% $\pm$ s.e.m.)	0	0	91 $\pm$ 0.6	83 $\pm$ 1.4	0	0	0	0
HIF-2 $\alpha$ +EPO (% $\pm$ s.e.m.)	0	0	51 $\pm$ 9.5	28 $\pm$ 3.2	0	0	0	0

Abbreviations: EPO, erythropoietin; FG, FG-4497; HIF, hypoxia-inducible factor; IC, interstitial cell; VE, vehicle.

Quantitative evaluations of superficial and juxtamedullary (deep) regions of the cortex from VE and FG-treated rats. Signals located in ICs or tubules within deep vs. superficial cortex were evaluated. Upper three lines: Cell counts normalized for sectional area. Lower three lines: Colocalization of EPO and HIF signal as quantified on adjacent mirror sections. Line 5 (EPO+HIF-2 $\alpha$ ) specifies the percentage of EPO mRNA-positive cells also showing a HIF-2 $\alpha$  signal. Line 6 (HIF-2 $\alpha$  + EPO) refers to the percentage of HIF-2 $\alpha$ -immunoreactive interstitial cells also expressing EPO mRNA.

Data are means  $\pm$  s.e.m.;  $n=4$  per group.

To validate our model of FG-4497-induced EPO expression, we compared renal cortical EPO mRNA abundance in FG-4497-treated animals with that in animals subjected to isobaric hypoxic hypoxia with a FiO<sub>2</sub> of 0.08. Hypoxia and FG-4497 treatments caused increases in renal cortical EPO mRNA content in a similar range; however, increases were more pronounced in hypoxic rats (26  $\pm$  4-fold of control;  $P<0.05$ ) than in FG-4497-treated rats (8.5  $\pm$  1-fold of control;  $P<0.05$ ) (Figure 6).

## DISCUSSION

Our results, for the first time, show colocalization of EPO mRNA and HIF-2 $\alpha$ -immunoreactive signal in interstitial fibroblasts of the renal cortex under the HIF-stabilizing condition of pharmacologically induced HIF-PHD inhibition. This measure was suitable to induce EPO and HIF cellular signals reliably and reproducibly, corresponding to the effects of established, biologically or chemically induced systemic hypoxia. A comparison with hypoxia showed that the obtained increases in EPO mRNA were in a similar range, although more pronounced in hypoxic, than in FG-4497-treated, rats; this shows that the applied dose of FG-4497 (50 mg/kg) caused an effect comparable with hypoxia in the mild to mid-grade range.<sup>29</sup> Marked increases in EPO mRNA and both HIF- $\alpha$  isoforms upon FG-4497 treatment were consistent with those of previous studies using HIF-PHD inhibitors.<sup>8–11</sup> The distribution of EPO mRNA in FG-4497-treated animals was similar to that observed in animals exposed to systemic hypoxia.<sup>20–25</sup> The cellular localization of HIF- $\alpha$  isoforms corresponded to that obtained in animals that had been subjected to hypoxia or to the nonspecific inhibitor of HIF prolyl hydroxylation, cobaltous chloride.<sup>26–28</sup> Our analysis of serial sections stained for EPO mRNA and HIF- $\alpha$  isoforms showed that the majority of EPO-expressing fibroblasts, which showed highest density in the juxtamedullary portions of the cortical labyrinth, also displayed HIF-2 $\alpha$  staining. We could further show that HIF-2 $\alpha$  accumulation was also localized in a fraction of capillary endothelial cell nuclei of the peritubular interstitium. Nonetheless, EPO mRNA was principally absent in these cells, which is in agreement with the outcome of a recent

transgenic approach.<sup>24</sup> Furthermore, EPO and HIF-1 $\alpha$  signals were entirely separated, as HIF-1 $\alpha$  signals were detected only in tubular epithelia. This is in concordance with previous work,<sup>8,26</sup> and in general, earlier data on an epithelial localization of renal EPO synthesis in the adult organism have not received further support from more recent approaches.<sup>24,30,31</sup>

Our findings are thus consistent with an important role of HIF-2 $\alpha$  in the regulation of EPO mRNA expression of the adult kidney. The fibroblast nature of HIF-2 $\alpha$ -stained interstitial cells was confirmed by concomitant 5'NU immunostaining and by the absence of major histocompatibility complex II staining, signifying that dendritic cells or macrophages were not involved.<sup>32</sup> It is important to note that HIF-2 $\alpha$  signals—similar to EPO signals—were only found in a fraction of 5'NU-positive fibroblasts. Furthermore, only a subset of the HIF-2 $\alpha$ -positive cells showed concomitant EPO expression, which implies that the cellular accumulation of HIF-2 $\alpha$  *per se* is not sufficient to induce EPO transcription. Therefore, it is likely that further regulatory, as yet unidentified components must act in concert with HIF-2 $\alpha$  to produce the typical, restricted distribution pattern of EPO mRNA-expressing fibroblasts. A differential regulation of these components could also be relevant for the HIF-1 $\alpha$ -dependent stimulation of EPO transcription under certain conditions.<sup>13,15,16</sup> Candidates for these components may be GATA transcription factors, hepatocyte nuclear factor 4, nuclear factor  $\kappa$ B, and various protein kinases, which have all been shown to modulate EPO.<sup>2,24,33–35</sup> Their involvement in the restriction of EPO in health and disease, as well as during development, must be resolved to advance mechanistic insights into the renal response to hypoxia. HIF-PHD inhibitors may serve as useful tools in this study. Our data provide no compelling evidence that the subset of interstitial fibroblasts coexpressing EPO mRNA and HIF-2 $\alpha$  is a cell type of its own; rather, available evidence favors the concept of a highly flexible potential to synthesize EPO that is not necessarily restricted to the innermost renal cortex.<sup>23,24,36</sup>

In conclusion, we have shown that treatment with the HIF-PHD inhibitor FG-4497 significantly increased abundances in renal HIF- $\alpha$  protein and EPO mRNA levels.



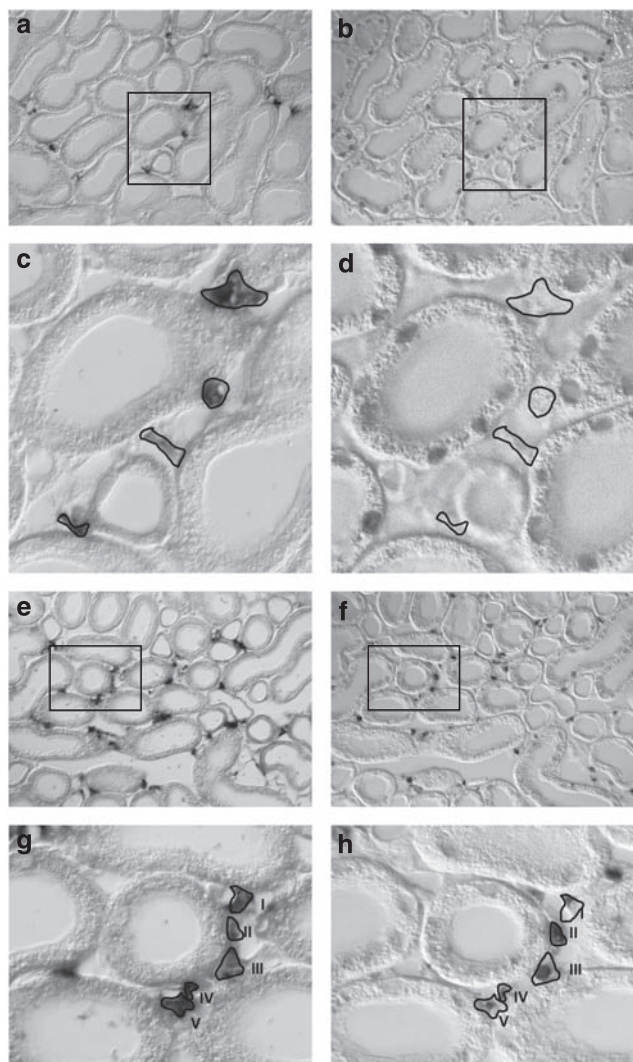


**Figure 2 | EPO mRNA colocalizes with HIF-2 $\alpha$  but not with HIF-1 $\alpha$ .** (a,c,e,g) Comparative localization of EPO mRNA, (b,d) HIF-1 $\alpha$  immunoreactivity, and (f,h) HIF-2 $\alpha$  immunoreactivity on consecutive (mirror) sections of FG-4497-treated tissues; images are arranged pairwise. (a-d) EPO *in situ* signals and HIF-1 $\alpha$  immunoreactivity are not coexpressed as shown in the overview (a and b) and detail (c and d; boxed in overviews). In contrast, EPO *in situ* signals and HIF-2 $\alpha$  immunoreactivity are frequently coexpressed in cortical interstitial fibroblasts as shown by the overview (e and f) and detail (g and h; boxed in overviews). Circumferences of EPO-expressing fibroblasts are marked for clarity and numbered (I-V) in panels g and h. Original magnification  $\times 400$ . EPO, erythropoietin; HIF, hypoxia-inducible factor.

The novel findings in our study are based on cellular colocalization strategies and include (1) the demonstration of HIF-2 $\alpha$  expression in cortical interstitial fibroblasts and endothelial cells of the kidney and (2) the documentation that cellular EPO mRNA expression was restricted to cortical interstitial fibroblasts and colocalized with HIF-2 $\alpha$ , but not with HIF-1 $\alpha$ . These findings supplement functional studies demonstrating a prominent role of HIF-2 $\alpha$  in the regulation

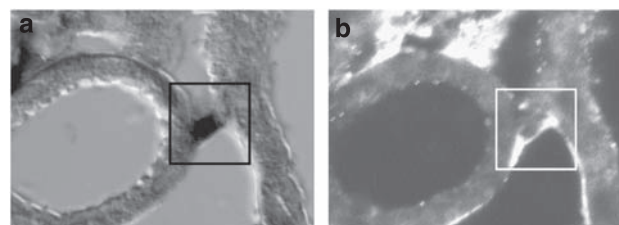


**Figure 3 | EPO mRNA colocalizes with ecto-5'-nucleotidase.** (a) Representative localization of EPO mRNA and (b) the fibroblast marker, ecto-5'-nucleotidase (5'NU); double staining on the same section from FG-4497-treated tissues. All EPO-expressing cells are located in the cortical interstitium and also stain positive for 5'NU. Boxes in panels a and b highlight the typical staining pattern. Original magnification  $\times 400$ . EPO, erythropoietin.

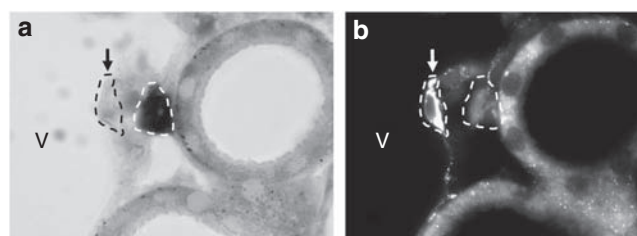


**Figure 4 | EPO mRNA does not colocalize with caveolin-1.** (a) Comparative localization of EPO mRNA and (b) the endothelial marker, caveolin (Cav)-1; double staining on the same section from FG-4497-treated tissues. EPO mRNA and Cav-1 show complete separation of signals, indicating that EPO is not expressed in endothelial cells. Cell circumferences are marked for clarity. Arrows point to an endothelial cell. V, vein. Original magnification  $\times 400$ . EPO, erythropoietin.

of renal EPO expression. Our data will further be relevant for clinical trials testing HIF-stabilizing agents for the therapeutic modulation of EPO.

## MATERIALS AND METHODS

### General

The HIF-PHD inhibitor FG-4497 was provided by FibroGen (San Francisco, CA, USA) and used as described previously.<sup>8</sup> Briefly, FG-4497 was dissolved by sonification in an alkalized 5% glucose solution (10 mg/dl; pH 8.7) and applied intravenously at a dose of 50 mg/kg body weight. This dose has been previously shown to be well tolerated and to markedly increase plasma EPO levels in mice and Rhesus Macaques within 4–6 h.<sup>8–11</sup>

### Animal models and tissue preparation

Animal studies were conducted in accordance with the German law for animal protection (reference nos G0014/07 and G0189/07 of the Berlin Senate) and NIH policies. Adult male Sprague-Dawley rats (body weight 250 g) were used throughout the study. FG-4497 or vehicle was applied intravenously after anesthesia with isoflurane (inhalation) or intraperitoneal injection of ketamine (100 mg/kg intraperitoneally). Rats were subsequently allowed to regain consciousness for the treatment period of 6 h. After treatment,

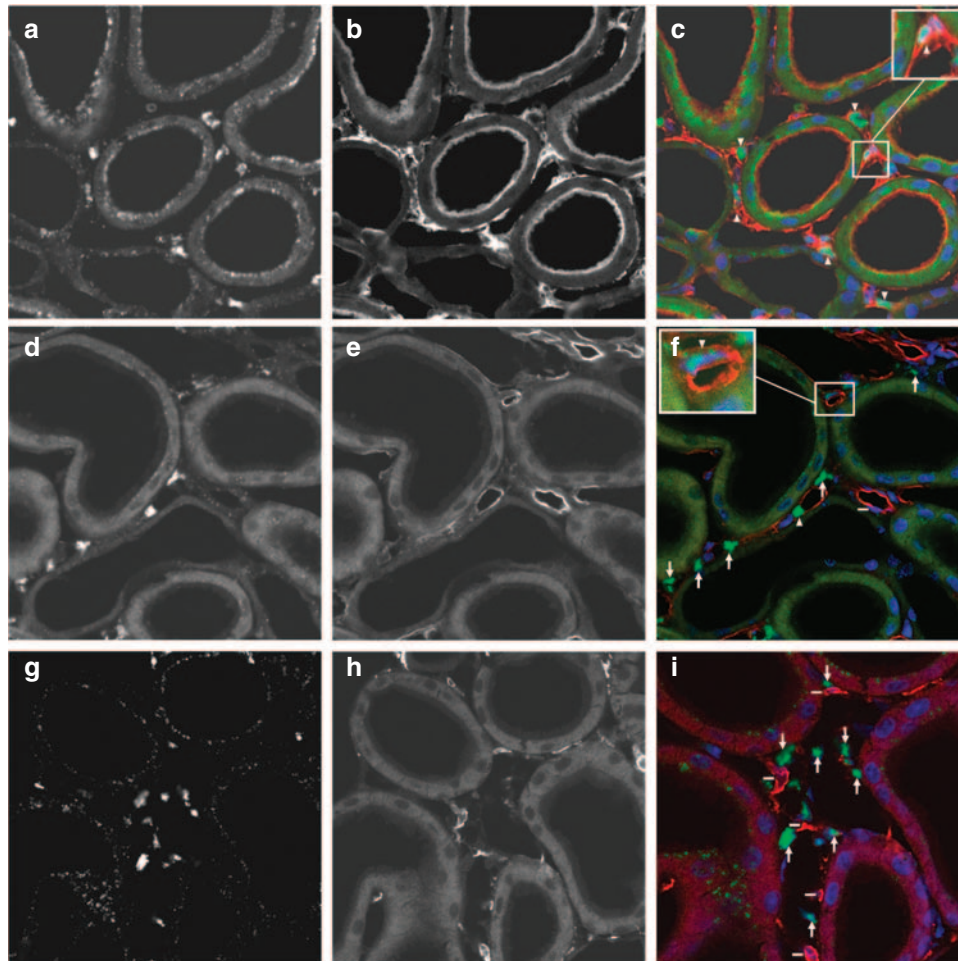


**Figure 5 | HIF-2 $\alpha$  immunoreactivity colocalizes with ecto-5'-nucleotidase and RECA-1, but not with MHC II. (a,d,g)** Comparative localization of HIF-2 $\alpha$  and **(b)** 5'NU, **(e)** the endothelial marker RECA-1, and **(h)** MHC II; double staining on the same sections from FG-4497-treated tissues. In the merged color images **(c,f,i)**, green signals mark HIF-2 $\alpha$  and red signals indicate 5'NU **(c)**, RECA-1 **(f)**, and MHC II **(i)**. The majority of HIF-2 $\alpha$ -immunoreactive cortical interstitial cells also stain positive for 5'NU (arrowheads). Inserts show high-power magnifications of a HIF-2 $\alpha$ -positive interstitial fibroblast **(c)** and a HIF-2 $\alpha$ -immunoreactive endothelial cell **(f)**. Arrowheads indicate coexpression of HIF-2 $\alpha$  and the respective marker, arrows point to HIF-2 $\alpha$ -positive cells not expressing the respective marker, and bars indicate cells expressing the respective marker, but not HIF-2 $\alpha$ . Original magnification  $\times 400$ . HIF-2 $\alpha$ , hypoxia-inducible factor-2 $\alpha$ ; MHC II, major histocompatibility complex II; 5'NU, ecto-5'-nucleotidase; RECA-1, rat endothelial cell antigen-1.

**Table 2 | Numerical evaluation of HIF-2 $\alpha$ - and specific marker-labeled cells**

	Interstitial cells (per $\times 400$ field)	HIF-2 $\alpha$ pos. (per $\times 400$ field)	HIF-2 $\alpha$ and marker (%)
RECA-1	18 $\pm$ 3.3	6.5 $\pm$ 1.5	25 $\pm$ 5.6
Ecto-5'-nucleotidase	17 $\pm$ 1.35	6.9 $\pm$ 0.7	74 $\pm$ 9.7
MHC II	17 $\pm$ 1.74	6.6 $\pm$ 1.5	0

Abbreviations: DAPI, 4'-6-diaminidine-2-phenyl indole; HIF-2 $\alpha$ , hypoxia-inducible factor-2 $\alpha$ ; MHC II, major histocompatibility complex II; pos., positive; RECA-1, rat endothelial cell antigen-1.

Cells were counted per optical field as viewed on double-stained sections from FG-4497-treated tissues. Categories refer to the absolute number of interstitial cells identified by DAPI nuclear stain, number of HIF-2 $\alpha$ -positive cells, and percentage of the HIF-2 $\alpha$ -positive cells that co-express one of the markers listed. Data are means  $\pm$  s.e.m.

the kidneys were either perfusion-fixed with 3% paraformaldehyde through the abdominal aorta ( $n = 4$  per group)<sup>20</sup> or processed for mRNA isolation ( $n = 5$  per group). In a parallel approach, rats were

subjected to isobaric hypoxic hypoxia in a sealed hypoxic chamber (FiO<sub>2</sub> 0.08; 6 h;  $n = 5$  per group), anesthetized after the treatment period, killed, and the kidneys were harvested for mRNA isolation. The renal cortex was separated from the medulla at  $-30^\circ\text{C}$  using a sterile razor blade. Tissue samples were processed for mRNA isolation using the Qiagen RNeasy kit (Qiagen, Hilden, Germany). cDNA was prepared using the Biotin cDNA synthesis kit (Biotin, London, UK). Renal EPO mRNA content was determined in FG-4497- and hypoxia-treated animals by Taqman real-time PCR using an Applied Biosystems 7500 Fast Real-Time PCR system and the murine EPO probe Mm\_01202755 (Applied Biosystems, Darmstadt, Germany). Glyceraldehyde-3-phosphate dehydrogenase content was determined simultaneously and served as a loading control.

For localization studies, renal EPO mRNA expression was detected by nonradioactive mRNA *in situ* hybridization, with a probe covering base pairs 312–602 of rat EPO cDNA (NM\_0171001). HIF- $\alpha$  immunostaining was performed using established antisera and a high-amplification technique.<sup>8,12,27</sup>

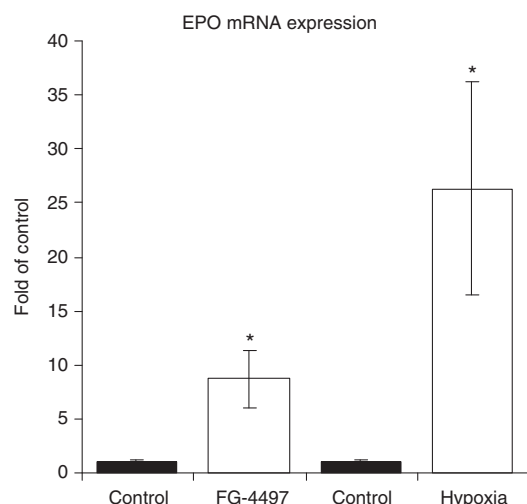


**Figure 6 | FG-4497 treatment and hypoxia induce renal EPO mRNA expression.** Cortical extracts of FG-4497- or hypoxia-treated rats were analyzed by TaqMan real-time PCR for EPO mRNA expression. Data are means  $\pm$  s.e.m. ( $n = 5$ ); \* $P < 0.05$ . EPO, erythropoietin.

Colocalization of EPO mRNA and HIF-2 $\alpha$  protein was studied on consecutive 3- $\mu$ m-thick paraffin sections; these were analyzed at their mirror surfaces and the images reoriented electronically. Cell counting was performed in the deep vs superficial halves of the cortex on sections stained for the respective HIF- $\alpha$  isoforms and EPO mRNA. Sections were examined using a Leica DMRB microscope equipped with an interference contrast module (Leica, Wetzlar, Germany). Images were acquired using a SPOT RT 2.3.0 digital camera (Diagnostic Instruments, Sterling Heights, MI, USA) and the MetaVue imaging System (Molecular Devices, Downingtown, PA, USA). To optimize the resolution of overview micrographs, two adjacent  $\times 100$  pictures of each staining were acquired and subsequently aligned electronically.

Characterization of EPO-expressing cortical interstitial cells was performed by double labeling EPO mRNA-stained sections with antibodies against 5'NU (rabbit anti-CD73; kind gift from Michel LeHir, Zurich, Switzerland) for interstitial fibroblasts,<sup>20,32</sup> and caveolin-1 (Santa Cruz Antibodies, Santa Cruz, CA, USA) for endothelial cells.<sup>37</sup> HIF-2 $\alpha$ -immunoreactive cortical interstitial cells were characterized by double-staining procedures using mouse monoclonal anti-5'NU (BD Pharmingen, Heidelberg, Germany),<sup>38</sup> the endothelial cell marker RECA-1 (ABD Serotec, Oxford, UK),<sup>39</sup> or the dendritic cell marker major histocompatibility complex II (Harlan Sera-lab, Belton, UK).<sup>32</sup> For double labeling, 6- $\mu$ m-thick cryostat sections were first stained for RECA-1, 5'NU, or major histocompatibility complex II according to standard protocols. Bound antibody was detected using a Cy3-labeled donkey anti-mouse secondary antibody (Dianova, Hamburg, Germany). After completion of the first staining procedure, sections were postfixed for 10 min using 3% paraformaldehyde in phosphate-buffered saline. The sections were subsequently subjected to HIF-2 $\alpha$  immunostaining using the high-amplification technique.<sup>27</sup> Cy2-conjugated streptavidin (Dianova) was used for detection. Nuclei were stained with DAPI (4'-6-diaminidino-2-phenyl indole; Sigma, Sigma-Aldrich, Munich, Germany). Sections were analyzed under a LSM5 Exciter confocal microscope (Zeiss, Jena, Germany). To

quantify the extent of colocalization of HIF-2 $\alpha$  with the different markers, 10 micrographs of the cortical interstitium, taken at random from FG-4497-treated rats ( $n = 4$ ), were analyzed (magnification  $\times 400$ ).

#### Analysis of data

Results were evaluated using routine parametric descriptive statistics. Groups were compared with the unpaired  $t$ -test. A probability level of  $P < 0.05$  was accepted as significant. Values are given as means  $\pm$  s.e.m.

#### DISCLOSURE

LAF, MA, and SJK are employees of FibroGen Inc. All of the other authors declared no competing interests.

#### ACKNOWLEDGMENTS

The study was supported in part by a grant from the Israeli Science Foundation (#1473/08). We thank Anna Gruber, Frauke Grams, and Petra Landmann for their expert technical assistance. The content of this paper has been presented as an oral communication at the Eighth International Luebeck Conference 'Pathophysiology and Pharmacology of Erythropoietin and other Hemopoietic Growth Factors,' University of Luebeck, Germany, 30 July to 1 August 2009.

#### REFERENCES

- Koury MJ, Bondurant MC, Graber SE *et al.* Erythropoietin messenger RNA levels in developing mice and transfer of 125I-erythropoietin by the placenta. *J Clin Invest* 1988; **82**: 154–159.
- Stockmann C, Fandrey J. Hypoxia-induced erythropoietin production: a paradigm for oxygen-regulated gene expression. *Clin Exp Pharmacol Physiol* 2006; **33**: 968–979.
- Epstein AC, Gleadle JM, McNeill LA *et al.* C. elegans EGL-9 and mammalian homologs define a family of dioxygenases that regulate HIF by prolyl hydroxylation. *Cell* 2001; **107**: 43–54.
- Jaakkola P, Mole DR, Tian YM *et al.* Targeting of HIF- $\alpha$  to the von Hippel-Lindau ubiquitylation complex by O<sub>2</sub>-regulated prolyl hydroxylation. *Science* 2001; **292**: 468–472.
- Ivan M, Haberberger T, Gervasi DC *et al.* Biochemical purification and pharmacological inhibition of a mammalian prolyl hydroxylase acting on hypoxia-inducible factor. *Proc Natl Acad Sci USA* 2002; **99**: 13459–13464.
- Safran M, Kim WY, O'Connell F *et al.* Mouse model for noninvasive imaging of HIF prolyl hydroxylase activity: assessment of an oral agent that stimulates erythropoietin production. *Proc Natl Acad Sci USA* 2006; **103**: 105–110.
- Warnecke C, Griethe W, Weidemann A *et al.* Activation of the hypoxia-inducible factor-pathway and stimulation of angiogenesis by application of prolyl hydroxylase inhibitors. *FASEB J* 2003; **17**: 1186–1188.
- Rosenberger C, Rosen S, Shina A *et al.* Activation of hypoxia-inducible factors ameliorates hypoxic distal tubular injury in the isolated perfused rat kidney. *Nephrol Dial Transplant* 2008; **11**: 3472–3478.
- Hsieh MM, Linde NS, Wynter A *et al.* HIF prolyl hydroxylase inhibition results in endogenous erythropoietin induction, erythrocytosis, and modest fetal hemoglobin expression in rhesus macaques. *Blood* 2007; **110**: 2140–2147.
- Robinson A, Keely S, Karhausen J *et al.* Mucosal protection by hypoxia-inducible factor prolyl hydroxylase inhibition. *Gastroenterology* 2008; **134**: 145–155.
- Schneider C, Krischke G, Keller S *et al.* Short-term effects of pharmacologic HIF stabilization on vasoactive and cytotoxic factors in developing mouse brain. *Brain Res* 2009; **1280**: 43–51.
- Warnecke C, Zaborowska Z, Kurreck J *et al.* Differentiating the functional role of hypoxia-inducible factor (HIF)-1 $\alpha$  and HIF-2 $\alpha$  (EPAS-1) by the use of RNA interference: erythropoietin is a HIF-2 $\alpha$  target gene in Hep3B and Kelly cells. *FASEB J* 2004; **18**: 1462–1464.
- Yeo EJ, Cho YS, Kim MS *et al.* Contribution of HIF-1 $\alpha$  or HIF-2 $\alpha$  to erythropoietin expression: in vivo evidence based on chromatin immunoprecipitation. *Ann Hematol* 2008; **87**: 11–17.
- Scortegagna M, Morris MA, Oktay Y *et al.* The HIF family member EPAS1/HIF-2 $\alpha$  is required for normal hematopoiesis in mice. *Blood* 2003; **102**: 1634–1640.



15. Yu AY, Shimoda LA, Iyer NV *et al.* Impaired physiological responses to chronic hypoxia in mice partially deficient for hypoxia-inducible factor 1 $\alpha$ . *J Clin Invest* 1999; **103**: 691–696.
16. Takeda K, Aguila HL, Parikh NS *et al.* Regulation of adult erythropoiesis by prolyl hydroxylase domain proteins. *Blood* 2008; **111**: 3229–3235.
17. Gruber M, Hu CJ, Johnson RS *et al.* Acute postnatal ablation of Hif-2 $\alpha$  results in anemia. *Proc Natl Acad Sci USA* 2007; **104**: 2301–2306.
18. Rankin EB, Biju MP, Liu Q *et al.* Hypoxia-inducible factor-2 (HIF-2) regulates hepatic erythropoietin in vivo. *J Clin Invest* 2007; **117**: 1068–1077.
19. Percy MJ, Furlow PW, Lucas GS *et al.* A gain-of-function mutation in the HIF2A gene in familial erythrocytosis. *N Engl J Med* 2008; **358**: 162–168.
20. Bachmann S, Le Hir M, Eckardt KU. Co-localization of erythropoietin mRNA and ecto-5'-nucleotidase immunoreactivity in peritubular cells of rat renal cortex indicates that fibroblasts produce erythropoietin. *J Histochem Cytochem* 1993; **41**: 335–341.
21. Koury ST, Bondurant MC, Semenza GL *et al.* The use of in situ hybridization to study erythropoietin gene expression in murine kidney and liver. *Microsc Res Tech* 1993; **25**: 29–39.
22. Maxwell PH, Osmond MK, Pugh CW *et al.* Identification of the renal erythropoietin-producing cells using transgenic mice. *Kidney Int* 1993; **44**: 1149–1162.
23. Koury ST, Koury MJ, Bondurant MC *et al.* Quantitation of erythropoietin-producing cells in kidneys of mice by in situ hybridization: correlation with hematocrit, renal erythropoietin mRNA, and serum erythropoietin concentration. *Blood* 1989; **74**: 645–651.
24. Obara N, Suzuki N, Kim K *et al.* Repression via the GATA box is essential for tissue-specific erythropoietin gene expression. *Blood* 2008; **111**: 5223–5232.
25. Semenza GL, Koury ST, Nejfelt MK *et al.* Cell-type-specific and hypoxia-inducible expression of the human erythropoietin gene in transgenic mice. *Proc Natl Acad Sci USA* 1991; **88**: 8725–8729.
26. Wiesener MS, Jurgensen JS, Rosenberger C *et al.* Widespread hypoxia-inducible expression of HIF-2 $\alpha$  in distinct cell populations of different organs. *FASEB J* 2003; **17**: 271–273.
27. Rosenberger C, Mandriota S, Jurgensen JS *et al.* Expression of hypoxia-inducible factor-1 $\alpha$  and -2 $\alpha$  in hypoxic and ischemic rat kidneys. *J Am Soc Nephrol* 2002; **13**: 1721–1732.
28. Rosenberger C, Griethe W, Gruber G *et al.* Cellular responses to hypoxia after renal segmental infarction. *Kidney Int* 2003; **64**: 874–886.
29. Eckardt KU, Ratcliffe PJ, Tan CC *et al.* Age-dependent expression of the erythropoietin gene in rat liver and kidneys. *J Clin Invest* 1992; **89**: 753–760.
30. Loya F, Yang Y, Lin H *et al.* Transgenic mice carrying the erythropoietin gene promoter linked to lacZ express the reporter in proximal convoluted tubule cells after hypoxia. *Blood* 1994; **84**: 1831–1836.
31. Kishore BK, Isaac J, Westenfelder C. Administration of poly-D-glutamic acid induces proliferation of erythropoietin-producing peritubular cells in rat kidney. *Am J Physiol Renal Physiol* 2007; **292**: F749–F761.
32. Kaissling B, Le Hir M. Characterization and distribution of interstitial cell types in the renal cortex of rats. *Kidney Int* 1994; **45**: 709–720.
33. Galson DL, Tsuchiya T, Tendler DS *et al.* The orphan receptor hepatic nuclear factor 4 functions as a transcriptional activator for tissue-specific and hypoxia-specific erythropoietin gene expression and is antagonized by EAR3/COUP-TF1. *Mol Cell Biol* 1995; **15**: 2135–2144.
34. La Ferla K, Reimann C, Jelkmann W *et al.* Inhibition of erythropoietin gene expression signaling involves the transcription factors GATA-2 and NF-kappaB. *FASEB J* 2002; **16**: 1811–1813.
35. Jelkmann W. Molecular biology of erythropoietin. *Intern Med* 2004; **43**: 649–659.
36. Eckardt KU, Koury ST, Tan CC *et al.* Distribution of erythropoietin producing cells in rat kidneys during hypoxic hypoxia. *Kidney Int* 1993; **43**: 815–823.
37. Komers R, Schutzer WE, Reed JF. Altered endothelial nitric oxide synthase targeting and conformation and caveolin-1 expression in the diabetic kidney. *Diabetes* 2006; **55**: 1651–1659.
38. Le Hir M, Hegyi I, Cueni-Loffing D *et al.* Characterization of renal interstitial fibroblast-specific protein 1/S100A4-positive cells in healthy and inflamed rodent kidneys. *Histochem Cell Biol* 2005; **123**: 335–346.
39. Duijvestijn AM, van Goor H, Klatter F *et al.* Antibodies defining rat endothelial cells: RECA-1, a pan-endothelial cell-specific monoclonal antibody. *Lab Invest* 1992; **66**: 459–466.